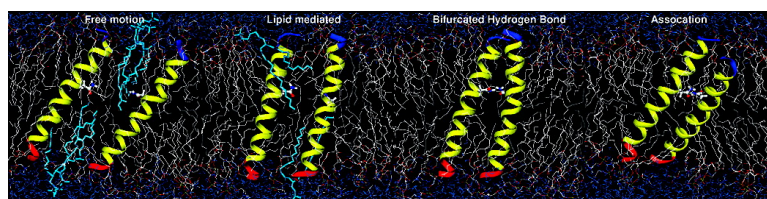


## Role of Hydrogen Bonding and Helix#Lipid Interactions in Transmembrane Helix Association

Jinhyuk Lee, and Wonpil Im

*J. Am. Chem. Soc.*, **2008**, 130 (20), 6456-6462 • DOI: 10.1021/ja711239h • Publication Date (Web): 19 April 2008

Downloaded from <http://pubs.acs.org> on February 8, 2009



### More About This Article

Additional resources and features associated with this article are available within the HTML version:

- Supporting Information
- Access to high resolution figures
- Links to articles and content related to this article
- Copyright permission to reproduce figures and/or text from this article

[View the Full Text HTML](#)

## Role of Hydrogen Bonding and Helix–Lipid Interactions in Transmembrane Helix Association

Jinhyuk Lee and Wonpil Im\*

Department of Molecular Biosciences and Center for Bioinformatics, The University of Kansas,  
2030 Becker Drive, Lawrence, Kansas 66047

Received December 19, 2007; E-mail: wonpil@ku.edu

**Abstract:** To explore the role of hydrogen bonding and helix–lipid interactions in transmembrane helix association, we have calculated the potential of mean force (PMF) as a function of helix–helix distance between two pVNVV peptides, a transmembrane model peptide based on the GCN4 leucine-zipper, in a dimyristoylphosphatidylcholine (DMPC) membrane. The peptide name pVNVV represents the interfacial residues in the heptad repeat of the dimer. The free energy decomposition reveals that the total PMF consists of two competing contributions from helix–helix and helix–lipid interactions. The direct, favorable helix–helix interactions arise from the specific contribution from the helix-facing residues and the generic contribution from the lipid-facing residues. The Asn residues in the middle of the helices show the most significant per-residue contribution to the PMF with various hydrogen bonding patterns as a function of helix–helix distance. Release of lipid molecules between the helices into bulk lipid upon helix association makes the helix–lipid interaction enthalpically unfavorable but entropically favorable. Interestingly, the resulting unfavorable helix–lipid contribution to the PMF correlates well with the cavity volume between the helices. The calculated PMF with an Asn-to-Val mutant (pVNVV → pVVVV) shows a dramatic free energy change upon the mutation, such that the mutant appears not to form a stable dimer below a certain peptide concentration, which is in good agreement with available experimental data of a peptide with the same heptad repeat. A transmembrane helix association mechanism and its implications in membrane protein folding are also discussed.

### Introduction

Membrane proteins are pharmaceutically important therapeutic targets because of their well-recognized contributions to ion transport and intra- and intercellular signaling pathways and their critical role in cell–cell recognition.<sup>1,2</sup> Determination of their structures and interactions can provide insights into the underlying pathologic mechanisms responsible for many human diseases, thus not only facilitating further functional studies but also potentially identifying strategies for rational drug design. Transmembrane (TM) domains of most membrane proteins consist of helices that interact with each other via inter- and intrahelix interactions, as well as with nonprotein membrane constituents. The delicate balance between these interacting forces may determine the structure and function of membrane proteins. Thus, the determination of molecular forces that govern the helix association in membranes will help us better understand and characterize the structure and function of membrane proteins at the atomic level.

Experimental studies on model peptides and statistical searches on structurally known membrane proteins have provided insights into important molecular interactions in TM helix association.<sup>3,4</sup> For instance, the TM domain of glycophorin A

(GpA) forms a right-handed dimer with close packing of the dimerization motif (G<sup>79</sup>V<sub>xx</sub>G<sup>83</sup>V).<sup>5</sup> The association is abolished when one of the Gly residues is mutated to Ala.<sup>6</sup> Similarly, Choma et al.<sup>7</sup> and Zhou et al.<sup>8</sup> independently designed membrane-soluble peptides, based on the soluble GCN4 leucine-zipper, that can form dimers or trimers by H-bonding between Asn residues in the middle of the TM helices. When Asn is replaced by Val, the association is shown to be abolished. These studies indicate that close packing and hydrophilic interactions between TM helices, which may be all competing with helix–lipid interactions, mediate the extent and specificity of TM helix association.<sup>4,9</sup> However, the detailed mechanisms and energetics of these interactions remain to be fully understood at the atomic level.

Several theoretical/computational studies have aimed to elucidate the detailed atomic interactions and driving forces of TM helix association.<sup>7,10–13</sup> Most notably, Hénin et al. recently calculated the dimerization free energy of the GpA TM region by calculating the potential of mean force (PMF) as a function of the distance between the centers of mass of the helices from

- (1) Drews, J. *Science* **2000**, *287*, 1960–1964.
- (2) Zheng, C. J.; Han, L. Y.; Yap, C. W.; Ji, Z. L.; Cao, Z. W.; Chen, Y. Z. *Pharm. Rev.* **2006**, *58*, 259–279.
- (3) Helms, V. *EMBO Rep.* **2002**, *3*, 1133–1138.
- (4) Senes, A.; Engel, D. E.; DeGrado, W. F. *Curr. Opin. Struct. Biol.* **2004**, *14*, 465–479.

- (5) MacKenzie, K. R.; Prestegard, J. H.; Engelman, D. M. *Science* **1997**, *276*, 131–133.
- (6) Fleming, K. G.; Engelman, D. M. *Proc. Natl. Acad. Sci. U.S.A.* **2001**, *98*, 14340–14344.
- (7) Choma, C.; Gratkowski, H.; Lear, J. D.; DeGrado, W. F. *Nat. Struct. Biol.* **2000**, *7*, 161–166.
- (8) Zhou, F. X.; Cocco, M. J.; Russ, W. P.; Brunger, A. T.; Engelman, D. M. *Nat. Struct. Biol.* **2000**, *7*, 154–160.
- (9) Schneider, D. *FEBS Lett.* **2004**, *577*, 5–8.

MD simulations in an explicit membrane.<sup>11</sup> The total PMF decomposition into helix–helix and helix–solvent contributions has greatly improved our understanding of the recognition and association mechanism of the GpA TM domain. Zhang and Lazaridis recently calculated the standard association free energy of GpA using an implicit membrane model, with consideration of translational, rotational, and conformational entropy contributions.<sup>12</sup> The calculated association free energy of GpA in micelles showed good agreement with the experimental value.

In the present study, we used a model peptide called pVNVV (acetyl-LLLL LLLL LLLL LLLVL LLLL VL-amine), where the peptide name pVNVV represents the interfacial residues in the heptad repeat of the dimer. The pVNVV is similar to MS1,<sup>7</sup> a designed membrane-soluble peptide based on the GCN4 leucine zipper (PDB 2ZTA),<sup>14</sup> but further simplified to focus on the role of the polar residue Asn in TM helix association. By utilizing a novel restraint potential for the helix–helix minimum distance (hereafter simply called the helix–helix distance or denoted by  $r_{\text{HH}}$ ),<sup>15</sup> we performed a total of  $\sim 1.1 \mu\text{s}$  umbrella sampling MD simulations to calculate the PMF as a function of  $r_{\text{HH}}$  between two pVNVV peptides in a dimyristoylphosphatidylcholine (DMPC) bilayer. Furthermore, the free energy change upon Asn-to-Val mutation (pVNVV  $\rightarrow$  pVVVV) was measured by calculating the free energy profile of pVVVV association from a total of  $\sim 0.6 \mu\text{s}$  umbrella sampling. The detailed structural features and energetic contributions of the Asn H-bonds and lipid molecules are presented and discussed, together with a possible TM helix association mechanism and its implications in membrane protein folding.

## Methods

An initial conformation of the associated pVNVV peptides was built, based on PDB 2ZTA (Leu5-Gly31), and shows a helix–helix distance of 8.7 Å and a crossing angle of 22° (left-handed dimer),<sup>14</sup> according to the definition used by Chothia et al.<sup>16</sup> All calculations were performed using the biomolecular simulation program CHARMM.<sup>17</sup> We used a time step of 2 fs for the NPAT (constant pressure, surface area, temperature) dynamics with the all-atom parameter set PARAM22 for proteins,<sup>18</sup> including the dihedral cross-term corrections (CMAP)<sup>19</sup> and a modified TIP3P water model,<sup>20</sup> as well as recently optimized lipid parameters for DMPC.<sup>21</sup> Although it would be better to perform NPT (constant pressure, surface tension, and temperature) dynamics in order to consider the change of the system area at different  $r_{\text{HH}}$ , we assume that the total area in each window would not be very different because each window was generated by increasing or decreasing the helix–helix distance of the associated dimer (see below). The

van der Waals interactions were smoothly switched off at 11–12 Å. To remove the artifact associated with truncation of electrostatic forces, electrostatic interactions were calculated using Particle-Mesh Ewald method with a mesh of  $64 \times 64 \times 64$  grid points,  $\kappa = 0.34 \text{ \AA}^{-1}$ , and a sixth-order B-spline interpolation.<sup>22</sup> All bond lengths involving hydrogen atoms were fixed using the SHAKE algorithm.<sup>23</sup>

The explicit membrane system consists of two pVNVV peptides, 128 DMPC lipid molecules, and 3835 water molecules. Using the so-called insertion method in Membrane Builder<sup>24</sup> at the CHARMM-GUI Web site (<http://www.charmm-gui.org>),<sup>25</sup> the associated peptides were first inserted into a hole in a pre-equilibrated DMPC bilayer. The hole size roughly corresponds to the cross-sectional area of the peptides. We carried out about 4.3 ns equilibration by imposing restraints to the peptide as well as the membrane constituents, as summarized in Table S1 in the Supporting Information. These restraint forces were slowly reduced as the equilibration progressed. To calculate the PMF as a function of helix–helix distance, a total of 57 windows were constructed from  $r_{\text{HH}} = 7 \text{ \AA}$  to  $r_{\text{HH}} = 20.75 \text{ \AA}$  every 0.25 Å and an additional distance at 10.375 Å. Although other choices can be made, we have used  $C_{\alpha}$  atoms to define the helical principal axis to calculate  $r_{\text{HH}}$ .<sup>15,16</sup> An initial structure in each window was generated by successively increasing  $r_{\text{HH}}$  of the equilibrated associated peptides to 20.75 Å or decreasing it to 7 Å by 0.25 Å every 50 ps by applying the helix–helix distance restraint potential<sup>15</sup> with a force constant of 500 kcal/(mol·Å<sup>2</sup>). Each system was then subjected to 4 ns equilibration and 15 ns production with a helix–helix distance force constant of 200 kcal/(mol·Å<sup>2</sup>) to restrain  $r_{\text{HH}}$  around each target value. For the PMF calculation of pVVVV, an Asn-to-Val mutant, we performed 10 ns production in each window by taking a coordinate set at 1 ns production of pVNVV umbrella sampling and replacing Asn by Val.

## Results and Discussion

**Total PMF.** Although other reaction coordinates could be chosen,<sup>11,26</sup> we calculated the PMF as a function of  $r_{\text{HH}}$  by utilizing the helix–helix distance restraint potential that we have recently developed.<sup>15</sup> The reasons are two-fold. First, the definition of  $r_{\text{HH}}$ , introduced by Chothia et al.,<sup>16</sup> has been widely used to characterize helix packing in proteins, and  $r_{\text{HH}}$  appears to be a natural reaction coordinate to study the helix–helix interactions in membranes. Second, since the restraint forces are exerted only on atoms that define the helical principal axis, each helix can rotate around the helical axis, depending on helix–helix or helix–lipid intermolecular interactions.<sup>15</sup>

Starting from the initial structure of pVNVV, we first generated 57 independent systems (windows) from  $r_{\text{HH}} = 7 \text{ \AA}$  to 20.75 Å (see Methods for details). Figure 1 shows the molecular structures at four different helix–helix distances. After 15 ns production in each window, the total PMF of pVNVV association,  $W(r_{\text{HH}})$ , was calculated by integrating the mean force  $\langle F(r_{\text{HH}}) \rangle_{r_{\text{HH}}}$  along  $r_{\text{HH}}$ , i.e.,

$$\frac{dW(r_{\text{HH}})}{dr_{\text{HH}}} = -\langle F(r_{\text{HH}}) \rangle_{r_{\text{HH}}} = \left\langle \frac{\partial U(r)}{\partial r_{\text{HH}}} \right\rangle_{r_{\text{HH}}} \quad (1)$$

where  $U(r)$  is the potential energy of the system.<sup>11,27–29</sup> Note that the Jacobian contribution related to the transformation of

- (10) Lagüe, P.; Zuckermann, M. J.; Roux, B. *Biophys. J.* **2001**, *81*, 276–284.
- (11) Hénin, J.; Pohorille, A.; Chipot, C. *J. Am. Chem. Soc.* **2005**, *127*, 8478–8484.
- (12) Zhang, J.; Lazaridis, T. *Biophys. J.* **2006**, *91*, 1710–1723.
- (13) Stockner, T.; Ash, W.; MacCallum, J.; Tieleman, D. *Biophys. J.* **2004**, *87*, 1650–1656.
- (14) O’Shea, E.; Klemm, J.; Kim, P.; Alber, T. *Science* **1991**, *254*, 539–544.
- (15) Lee, J.; Im, W. *J. Comput. Chem.* **2007**, *28*, 669–680.
- (16) Chothia, C.; Levitt, M.; Richardson, D. *J. Mol. Biol.* **1981**, *145*, 215–250.
- (17) Brooks, B. R.; Brucoleri, R. E.; Olafson, B. D.; States, D. J.; Swaminathan, S.; Karplus, M. *J. Comput. Chem.* **1983**, *4*, 187–217.
- (18) MacKerell, A. D., Jr. *J. Phys. Chem. B* **1998**, *102*, 3586–3616.
- (19) MacKerell, A. D., Jr.; Feig, M.; Brooks, C. L., III. *J. Comput. Chem.* **2004**, *25*, 1400–1415.
- (20) Jorgensen, W. L.; Chandrasekhar, J.; Madura, J. D.; Impey, R. W.; Klein, M. L. *J. Chem. Phys.* **1983**, *79*, 926–935.
- (21) Klauda, J.; Brooks, B., Jr.; Venable, R.; Pastor, R. *J. Phys. Chem. B* **2005**, *109*, 5300–5311.

- (22) Essmann, U.; Perera, L.; Berkowitz, M. L.; Darden, T.; Lee, H.; Pedersen, L. G. *J. Chem. Phys.* **1995**, *103*, 8577–8593.
- (23) Ryckaert, J. P.; Ciccolini, G.; Berendsen, H. J. C. *J. Comput. Chem.* **1977**, *23*, 327–341.
- (24) Jo, S.; Kim, T.; Im, W. *PLoS ONE* **2007**, *2*, e880.
- (25) Jo, S.; Kim, T.; Iyer, V. G.; Im, W. *J. Comput. Chem.* **2008**, . in press.
- (26) MacCallum, J. L.; Moghaddam, M. S.; Chan, H. S.; Tieleman, D. P. *Proc. Natl. Acad. Sci. U.S.A.* **2007**, *104*, 6206–6210.
- (27) Lee, J.; Im, W. *Chem. Phys. Lett.* **2007**, *441*, 132–135.

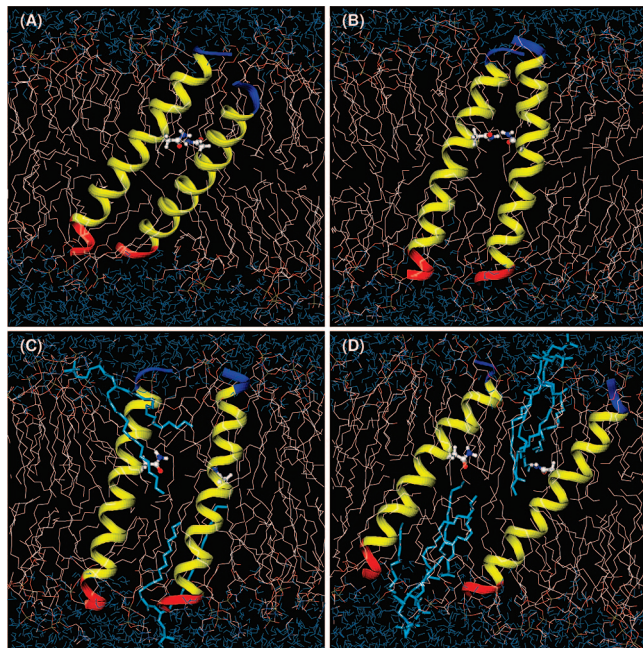


**Figure 1.** Molecular graphics views of explicit membrane systems at helix–helix distances of (A) 9.5, (B) 11.5, (C) 14, and (D) 18 Å. In each peptide, the N-terminus is blue, the C-terminus is red, and Asn is represented by ball-and-stick models. Lipid molecules between two helices are represented by thicker stick models. For clarity, some lipid molecules are removed from the front view.

the Cartesian coordinate into  $r_{HH}$  was not included in eq 1 because this contribution is not relevant to the helix association PMF. The mean forces along  $r_{HH}$  were calculated by projection of Cartesian forces onto the helix–helix distance vector,  $\mathbf{r}_{HH}$ .<sup>15</sup> Assuming that the helix–water contribution does not vary as a function of  $r_{HH}$ , the total PMF was calculated by integrating the mean forces from helix–helix and helix–lipid interactions. Such an assumption is justified by the fact that the helices are mostly embedded in the bilayers as shown in Figure 1, and also practical because the helix–water interactions appeared to be a very slowly converging component due to slow sampling along the helix tilt in membranes.<sup>30</sup> Figure 2A shows the resulting total PMF as a function of  $r_{HH}$ . The relative helix association free energy is estimated at  $-12.6 \pm 2.9$  kcal/mol by taking the difference between the plateau value around  $r_{HH} = 19.25$  Å and the minimum value at  $r_{HH} = 9.4$  Å. Although the distance is slightly increased in the membrane environment, the helix–helix distance at the minimum free energy is close to that of the GCN4 leucine zipper (PDB 2ZTA,  $r_{HH} = 8.7$  Å), which served as the basis for building the initial associated conformation of two pVNVV peptides.

There is no direct experimental measurement of the pVNVV association free energy. However, recent analytical ultracentrifugation experiments estimated a free energy change of  $\sim 6$  kcal/mol for MS1 including aqueous helical extensions in a DPC micelle.<sup>31</sup> Although the existence of the aqueous helices made it difficult to compare our result with the experimental value, it

is still worth stressing that the calculated association free energy ( $-7.8 \pm 2.9$  kcal/mol) in micelle environments appears to be reasonable after consideration of (1) the difference in the peptide/detergent ratio (1:150) corresponding to about 0.5 kcal/mol (see Influence of Concentration), (2) the translational and rotational entropy contribution, which is missing in the PMF calculation due to limited sampling, corresponding to about 3.0 kcal/mol,<sup>12</sup> and (3) the association free energy difference between micelles and bilayers, corresponding to about 1.3 kcal/mol.<sup>12</sup>

**PMF Decomposition.** The free energy decomposition based on eq 1 reveals that the total PMF in Figure 2A consists of two competitive contributions from helix–helix and helix–lipid interactions. As shown in Figure 2B, the free energy contribution from the direct helix–helix interaction appears to be screened by the helix–lipid interaction. Such a screening by solvent molecules, although the detailed shapes are different, is analogous to the case of ion–ion<sup>32</sup> and protein–protein interactions in solution.<sup>33</sup> As the helices approach each other, the attractive helix–helix interaction exceeds the opposing helix–lipid interaction, resulting in a stable pVNVV dimer.

To explore the contribution of each residue type, the direct helix–helix free energy profile (red line in Figure 2B) was further decomposed to the individual residue level (Leu, Val, and Asn), and the result is shown in Figure 2C. There are three Val residues in pVNVV that are located at the heptad repeats of the helix–helix interface in the initial coiled-coil dimer. Despite their nonpolar nature, steric clash between two  $\beta$ -branched side chains in Val makes their contribution repulsive when the helices are in contact ( $r_{HH} < 12.0$  Å). On the other hand, the overall contribution of 23 Leu residues in pVNVV makes a dominant (favorable) contribution to the helix association. Although Leu has a larger side chain than Val, the Leu residues (Leu1, Leu8, Leu15, and Leu22) at the helix–helix interface make a favorable contribution to the helix association, as shown in Figure 2C. Such different behaviors of interfacial Val and Leu residues result from the fact that Leu with one  $\beta$ -branched side chain has more freedom to adjust for better packing than Val does.<sup>34</sup> As shown in Figure 2C and Table 1, the non-interfacial Leu residues appear to dominate the direct helix–helix contribution to the total PMF in the case of pVNVV. However, the per-residue contributions from the interfacial and non-interfacial residues are  $-1.63$  (3 residues) and  $-0.59$  kcal/mol (19 residues), respectively. This analysis implies that the interfacial residues appear to play an important role in specific helix–helix association (e.g., single Asn contribution is  $-2.3$  kcal/mol, and single Leu contribution is  $-1.63$  kcal/mol), while the non-interfacial residues make a common/generic contribution to helix–helix association in membranes. The abundance of Leu in pVNVV might be one of the reasons why the calculated association free energy is lower than the experimental value measured for MS1. The Asn contribution is attractive and has two minima at  $r_{HH} = 9.8$  and  $11.9$  Å, which results from various Asn H-bonding patterns (see next section). Without the Asn H-bonding contribution, as shown in Figure 2D, it is apparent that the favorable van der Waals interactions, mostly from Leu residues, make dominant contributions to the direct helix–helix interactions. The electrostatic contribution without Asn H-

(28) Allen, T. W.; Andersen, O. S.; Roux, B. *Proc. Natl. Acad. Sci. U.S.A.* **2004**, *101*, 117–122.

(29) Lee, J.; Im, W. *Phys. Rev. Lett.* **2008**, *100*, 018103.

(30) Özdirekcan, S.; Etchebest, C.; Killian, J. A.; Fuchs, P. F. *J. Am. Chem. Soc.* **2007**, *129*, 15174–15181.

(31) Cristian, L.; Nanda, V.; Lear, J. D.; DeGrado, W. F. *J. Mol. Biol.* **2005**, *348*, 1225–1233.

(32) Masunov, A.; Lazaridis, T. *J. Am. Chem. Soc.* **2003**, *125*, 1722–1730.

(33) Jiang, L.; Gao, Y.; Mao, F.; Liu, Z.; Lai, L. *Proteins* **2002**, *46*, 190–196.

(34) Moitra, J.; Szilák, L.; Krylov, D.; Vinson, C. *Biochemistry* **1997**, *36*, 12567–12573.

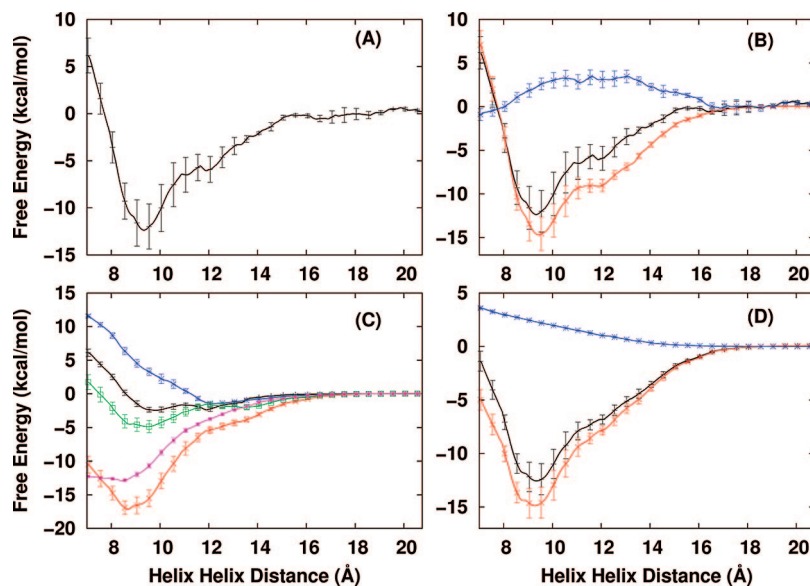


**Figure 2.** Total PMF of pVNVV as a function of  $r_{\text{HH}}$  and its decomposition into various contributions. (A) Total PMF for association of two pVNVV peptides. (B) Decomposition of the total PMF (black) into the direct helix–helix (red) and helix–lipid (blue) interactions. (C) Decomposition of the helix–helix contribution into contributions from each residue type: Asn (black), Leu (red), Leu at the helix–helix interface (green), Leu at the helix–lipid interface (violet), and Val (blue). (D) Decomposition of the helix–helix contribution (black) without the Asn H-bond contribution into contributions from van der Waals (red) and electrostatic interactions (blue). The Asn H-bond contribution was excluded by turning off all the interactions with the amino carbonyl group of the Asn side chain. The error bars of the PMF calculations were estimated from the PMFs calculated in three different time intervals by treating each 5 ns trajectory as an independent sampling.<sup>51</sup>

**Table 1.** Free Energy Decomposition in pVNVV<sup>a</sup>

$\Delta G_{\text{tot}}$	$\Delta G_{\text{HL}}$	$\Delta G_{\text{HH}}$	decomposition of $\Delta G_{\text{HH}}$				
			Asn	Val	Leu	Leu <sup>b</sup>	Leu <sup>c</sup>
$-12.6 \pm 2.9$	$2.2 \pm 0.6$ $3.2 \pm 0.9^d$	$-14.8 \pm 2.3$	$-2.3 \pm 0.4$	$3.6 \pm 0.6$ $1.2^e$	$-16.1 \pm 1.3$	$-4.9 \pm 1.0$ $-1.63^e$	$-11.2 \pm 0.3$ $-0.59^e$

<sup>a</sup> Energy in kcal/mol.  $\Delta G$  represents the association free energy change:  $\Delta G_{\text{tot}}$  (total),  $\Delta G_{\text{HL}}$  (helix–lipid contribution), and  $\Delta G_{\text{HH}}$  (helix–helix contribution). <sup>b</sup> Contribution from helix–helix interfacial Leu residues. <sup>c</sup> Contribution from lipid-facing Leu residues. <sup>d</sup> Maximum barrier of helix–lipid contribution at  $r_{\text{HH}} = 11.6 \text{ \AA}$ . <sup>e</sup> Per-residue contribution.

bonding is repulsive because the two helices behave like parallel macro-dipoles.<sup>35</sup>

**Asn Hydrogen Bonds.** The soluble GCN4 leucine zipper structure (PDB 2ZTA) shows one H-bond between two Asn side chains. Detailed structural analysis shown in Figure 3A, however, reveals a variety of H-bonding patterns of Asn residues in the membrane bilayer as a function of  $r_{\text{HH}}$ . As existed in PDB 2ZTA, the H-bond between Asn residues in the middle of the bilayer remains strong throughout the simulations at  $r_{\text{HH}} < 12 \text{ \AA}$  (black line in Figure 3A). Note that two Asn residues form a strong bifurcated H-bond when there is sufficient room to accommodate rotation of these side chains between the helices at  $11.0 \text{ \AA} < r_{\text{HH}} < 11.9 \text{ \AA}$  (see Figure 3C). Such a bifurcated H-bond has been suggested to play an important role in the dimerization of outer membrane phospholipase A (OMPLA) in *Escherichia coli* (PDB 1QD6).<sup>36,37</sup> As  $r_{\text{HH}}$  increases a bit further, the Asn–Asn H-bonds disappear at  $r_{\text{HH}} > 13.5 \text{ \AA}$ . However, this loss appears to be compensated by intra-peptide Asn–backbone H-bonds (green and violet lines in Figure 3A) to alleviate energetically unfavorable exposure of the polar side

chain to the membrane hydrophobic core. When  $r_{\text{HH}} < 10 \text{ \AA}$ , the Asn residue in one helix starts to make a H-bond with a backbone carbonyl oxygen in another helix, i.e., inter-peptide Asn–backbone H-bonding (red line in Figure 3A). This feature does not exist in PDB 2ZTA, probably because of water molecules close to the Asn residues in solution. Such an inter-peptide Asn–backbone H-bonding explains a highly conserved structure in rhodopsin<sup>38</sup> and facilitates a tight association in bovine cytochrome *c* oxidase.<sup>39</sup> Figure 3B,C shows the molecular pictures of various Asn H-bonding patterns.

The analysis of Asn H-bonding patterns clearly shows that the Asn contribution in the helix–helix interaction does not arise solely from the direct Asn–Asn H-bond. Instead, it suggests that the inter-peptide Asn–backbone H-bond can also contribute to the helix association. To better understand the contributions from these H-bonds, we calculated the contribution from the Asn–Asn H-bonds and the contribution from all Asn H-bonds as a function of  $r_{\text{HH}}$  (see Figure S1, Supporting Information). The former has a minimum of  $-2.6 \pm 0.65 \text{ kcal/mol}$  at  $r_{\text{HH}} = 11.9 \text{ \AA}$ . It becomes obvious from the H-bonding patterns in Figure 3A that the minimum results from the bifurcated Asn–Asn H-bond. While this contribution becomes repulsive at closer

(35) Gilson, M. K.; Honig, B. *Proc. Natl. Acad. Sci. U.S.A.* **1989**, *86*, 1524–1528.

(36) Snijder, H. J.; Ubarretxena-Belandia, I.; Blaauw, M.; Kalk, K. H.; Verheij, H. M.; Egmond, M. R.; Dekker, N.; Dijkstra, B. W. *Nature* **1999**, *401*, 717–721.

(37) Stanley, A. M.; Fleming, K. G. *J. Mol. Biol.* **2007**, *370*, 912–924.

(38) Palczewski, K.; Kumasaka, T.; Hori, T.; Behnke, C. A.; Motoshima, H.; Fox, B. A.; Trong, I. L.; Teller, D. C.; Okada, T.; Stenkamp, R. E.; Yamamoto, M.; Miyano, M. *Science* **2000**, *289*, 739–745.

(39) Adamian, L.; Liang, J. *Proteins* **2002**, *47*, 209–218.

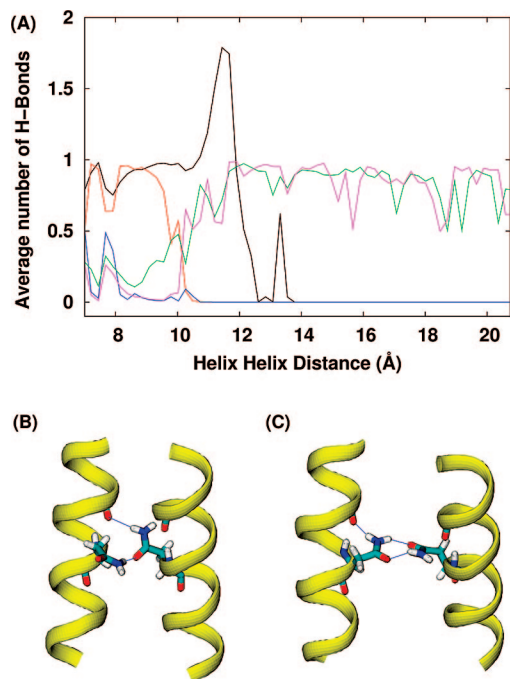


**Figure 3.** Various Asn H-bond patterns and their molecular graphics views. (A) Average number of H-bonds as a function of  $r_{HH}$ . There are three types of H-bonds: Asn-Asn H-bond (black), inter-peptide ASN backbone H-bond (red from helix A and blue from helix B), and intra-peptide ASN backbone H-bond (green from helix A and violet from helix B). The H-bond is defined by  $d \leq 2.8$  Å and  $120^\circ \leq \theta \leq 180^\circ$ , where  $d$  is the distance between donor and acceptor atoms and  $\theta$  is the H-bond angle. The donors are HD21 and HD22 of the Asn side chain and HN of the backbone, and the acceptors are OD1 of the Asn side chain and O of the backbone (CHARMM atom types). Shown at the bottom are the molecular graphics views of various H-bonds (blue lines) at (B)  $r_{HH} = 9$  Å and (C) 11 Å.

contacts ( $r_{HH} < 11$  Å), the inter-peptide Asn-backbone H-bonding dominates and makes the contribution from total Asn H-bonds attractive at the helix association distance, i.e., about  $-2.0 \pm 0.8$  kcal/mol.

**Lipid Contributions.** To investigate the role of lipid molecules in TM helix association, we calculated the number of lipid molecules surrounding two pVNVV helices as a function of  $r_{HH}$ . The result in Figure 4A represents the variation of solvation of the helices by lipid molecules upon helix association. The large number of lipid molecules in contact with the helices clearly reflects the complexity of helix–lipid interactions. As the helices approach each other, starting from  $r_{HH} = 18.0$  Å, the number decreases until  $r_{HH} = 12$  Å, where they are in contact. Figure 1C,D shows some of the lipid molecules between the helices. There are about nine lipid molecules that are released to bulk lipid upon helix association. Such a loss makes the helix–lipid interaction enthalpically unfavorable but entropically favorable because the helix–lipid interface is minimized upon the association.<sup>3,9</sup> As shown in Figure S2 (Supporting Information), these large competing forces mostly cancel each other and result in the small unfavorable helix–lipid contribution to the total PMF in Figure 2B. We have also examined the helix–lipid interactions at the residue level. As expected, the residues at the helix–helix interface (three Val and some Leu residues, but not Asn) make very unfavorable contributions upon helix association (see Figure S3, Supporting Information). In the case of Asn, there is no change because Asn residues prefer not to interact with lipid molecules by forming intra-peptide Asn-backbone H bonds, even when the helices are separated.

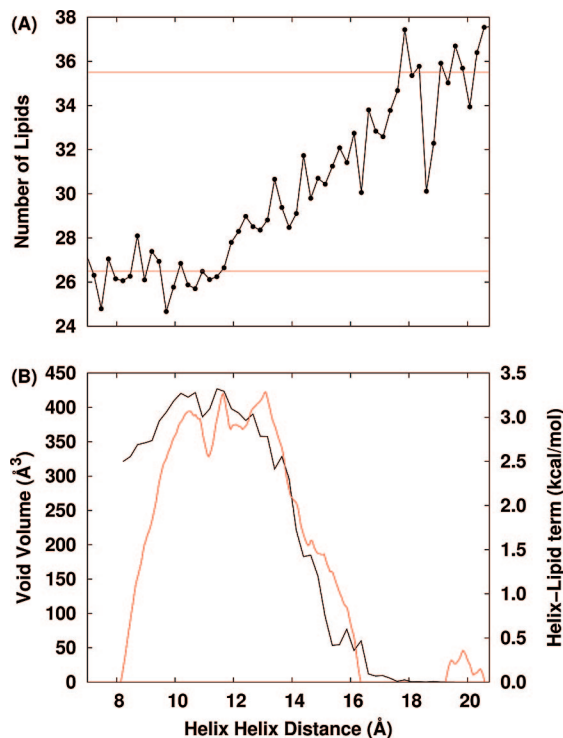


**Figure 4.** Solvation of pVNVV peptides by lipid molecules and cavity formation between the helices upon helix association. (A) Average number of lipid molecules surrounding two pVNVV helices as a function of  $r_{HH}$ . The number was counted if a lipid molecule was within 4.0 Å of any helix. The sudden decrease around  $r_{HH} = 18.75$  Å results from the fact that the helices around  $r_{HH} = 18.75$  Å have smaller tilt angles than others during the sampling period. (B) Average void volume (black) at the helix–helix interface and the helix–lipid contribution (red) as a function of  $r_{HH}$ . The volume was calculated by subtracting molecular volumes of individual helices from the total molecular volume of both helices using a probe radius of 2.5 Å, which approximately corresponds to the size of the methyl or methylene groups of lipid tails.<sup>52</sup>

Interestingly, the lipid-facing residues make very favorable contributions to the helix–lipid interactions. Although their interactions with lipid molecules remain enthalpically constant as a function of  $r_{HH}$ , these interactions become entropically favorable because the number of lipid configurations increases as  $r_{HH}$  decreases. Therefore, release of about nine lipid molecules upon helix association makes the interactions between interfacial residues and lipid molecules enthalpically unfavorable and the interactions between lipid-facing residues and lipid molecules entropically favorable (Figures S2 and S3). In the case of pVNVV, these contributions largely cancel each other and result in a small barrier, as shown in Figure 2B.

The gradual loss of lipid molecules upon association creates an instant void volume (cavity) between the helices in the membrane. People have envisioned that creating such a cavity in a medium requires a free energy cost and related the cost to the cavity volume or surface area with a phenomenological constant in a macroscopic sense.<sup>40,41</sup> Figure 4B shows the calculated cavity volume as a function of  $r_{HH}$ . Interestingly, when a phenomenological constant of  $7.6$  cal/(mol·Å<sup>3</sup>) is used as a free energy cost to create a void volume in the bilayer, the calculated volume is well correlated with the helix–lipid contribution to the total PMF. Note that the free energy cost of

(40) Eriksson, A. E.; Baase, W. A.; Zhang, X. J.; Heinz, D. W.; Blaber, M.; Baldwin, E. P.; Matthews, B. W. *Science* **1992**, 255, 178–183.

(41) Chandler, D. *Nature* **2005**, 437, 640–647.

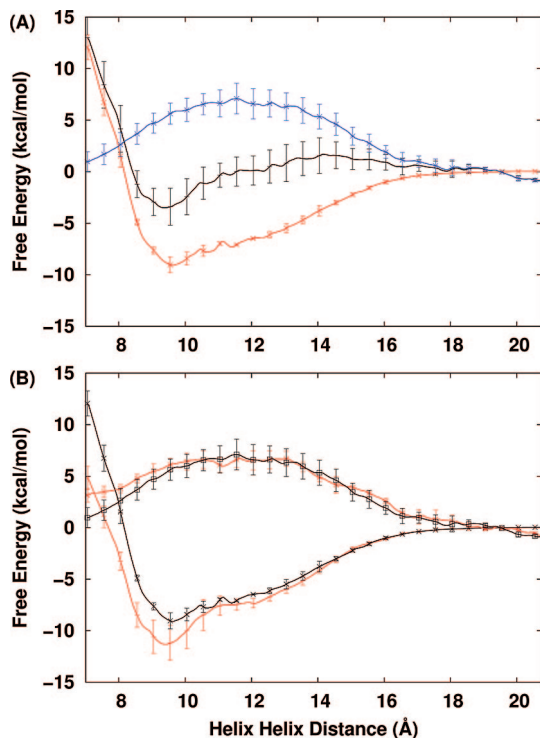


**Figure 5.** Total PMF of pVVVV as a function of  $r_{\text{HH}}$  and its decomposition into various contributions. (A) Decomposition of total PMF (black) of pVVVV into direct helix–helix (red) and helix–lipid (blue) interactions. PMFs were calculated from umbrella sampling MD simulation of pVVVV in a DMPC membrane. (B) Comparison of PMF from umbrella sampling of pVVVV (black) with the back-calculation from pVNVV PMFs (red).

creating a cavity inside soluble proteins has been experimentally estimated as  $24\text{--}33 \text{ cal}/(\text{mol} \cdot \text{Å}^3)$ .<sup>40</sup> In particular, the unfavorable helix–lipid interaction might be relevant to the so-called enthalpic folding barriers from the viewpoint of energetically unfavorable barriers along a folding reaction coordinate. The enthalpy barriers have been observed in MD simulations of dewetting of a melittin tetramer,<sup>42</sup> collapse of the BphC enzyme,<sup>43</sup> and association of two nonpolar helices in water.<sup>26</sup> While the helix association in water has a small barrier in the total PMF,<sup>26</sup> the pVNVV association in the membrane has no such a barrier in the total PMF because the competitive, attractive helix–helix interaction exceeds the helix–lipid interaction. Such a difference in two environments might arise from the fact that the free energy cost to create a cavity volume is much smaller in membranes than in water.

**Asn-to-Val Mutation.** Experimental studies suggest that the point mutation of Asn to Val abolishes the association of the designed peptides with the same heptad repeat as in pVNVV.<sup>7,8</sup> To better understand the influence of the mutation (pVNVV  $\rightarrow$  pVVVV) on the helix association, we have calculated the PMF as a function of  $r_{\text{HH}}$  between two pVVVV peptides in the DMPC bilayer in two different ways. First, the pVVVV PMF was calculated from 10 ns umbrella sampling in each window (see Methods for details). Second, we estimated the pVVVV PMF by subtracting the Asn contribution from, and adding a single Val contribution to, the pVNVV helix–helix and helix–lipid contributions at the residue level (Figures 2C and S3). Figure 5A shows the resulting PMF from the umbrella sampling

simulations and its decomposition into helix–helix and helix–lipid contributions. The association free energy of pV–VVV is estimated as  $-3.5 \pm 1.8 \text{ kcal/mol}$  by taking the difference between the PMF minimum at  $r_{\text{HH}} = 9.4 \text{ Å}$  and the plateau value between  $r_{\text{HH}} = 18$  and  $19.75 \text{ Å}$ . Therefore, the free energy change upon the mutation, which corresponds to the difference between association free energies of pVNVV ( $-12.6 \pm 2.9 \text{ kcal/mol}$  from Figure 2) and pVVVV ( $-3.5 \pm 1.8 \text{ kcal/mol}$ ), is  $9.1 \text{ kcal/mol}$ . Comparison between Figures 2B and 5A reveals that the single mutation decreases the favorable helix–helix contribution by  $6.0 \text{ kcal/mol}$  via losing favorable Asn contribution and adding unfavorable Val contribution (Figure 2C) and increases the unfavorable helix–lipid interaction by  $3.1 \text{ kcal/mol}$  via adding unfavorable Val contribution (Figure S3). These detailed analyses have yielded new insights into complicated influences of Asn-to-Val mutation on TM helix association. Figure 5B shows the comparison between the PMF calculation from umbrella sampling and the back-calculation from the pVNVV PMFs. Given the calculation errors as well as probable underestimation of unfavorable Val contributions at the Asn position, the agreement is very reasonable and clearly demonstrates that the mean force decomposition is a valid approach.

Is  $-3.5 \pm 1.8 \text{ kcal/mol}$  a reasonable estimation for pVVVV? To address this question, we now need to consider the influence of concentration and compare these results with available experiments.

**Influence of Concentration.** The helix association in membranes is influenced by the peptide concentration, i.e., the peptide/detergent ratio.<sup>44,45</sup> For instance, analytical ultracentrifugation and NMR experiments showed that the MS1 association dropped from 55.0% to 31.4% when the peptide/detergent ratio was changed from 1:125 to 1:1750.<sup>45</sup> To understand the influence of concentration on the association free energy, one has to consider the standard association free energy. However, it is often difficult to reasonably extrapolate the standard association free energy from experiments because a complex bilayer is not a sensible reference.<sup>44</sup> Theoretically, one can define the standard concentration (1 M) as the concentration of a monomer in a standard volume ( $1 \text{ L}/(6.023 \times 10^{23}) = 1660.3 \text{ Å}^3$ ).<sup>46</sup> In the case of our molecular system, the volume occupied by 128 lipids is equal to  $91694 \text{ Å}^3$ , calculated from  $L_x L_y L_z$ , where  $L_x = L_y = 64.84 \text{ Å}$  is the system length along  $X$  and  $Y$ , and  $L_z = 21.81 \text{ Å}$  corresponds to the average hydrophobic thickness of the DMPC bilayer, calculated from deuterium order parameters of lipid tails.<sup>47</sup> Following the definition of the standard concentration, our molecular system with a peptide/lipid ratio of 1:64 has a concentration of 36.2 mM. The standard free energy ( $\Delta G^\circ$ ) of pVNVV association becomes  $-14.6 \text{ kcal/mol}$  by  $\Delta G^\circ = \Delta G + k_B T \ln C$ , where  $\Delta G = -12.6 \text{ kcal/mol}$  from Figure 2 and  $C = 36.2 \text{ mM}$ . From a similar calculation,  $\Delta G^\circ$  of pVVVV association becomes  $-5.5 \text{ kcal/mol}$ . Based on  $\Delta G^\circ$ , we now can calculate pVNVV and pVVVV association free energies at any concentrations. Furthermore, by considering  $\Delta G_{\text{rot/trans}}$ , the translational and rotational entropy contribution (about  $3.0 \text{ kcal/mol}$ ),<sup>12</sup> and  $\Delta G_{\text{b-m}}$ , the association free energy difference between micelles

(42) Liu, P.; Huang, X.; Zhou, R.; Berne, B. J. *Nature* **2005**, *437*, 159–162.  
 (43) Zhou, R.; Huang, X.; Margulis, C. J.; Berne, B. J. *Science* **2004**, *305*, 1605–1609.

(44) Fisher, L. E.; Engelman, D. M.; Sturgis, J. N. *Biophys. J.* **2003**, *85*, 3097–3105.  
 (45) Gratkowski, H.; Dai, Q.; Wand, A. J.; DeGrado, W. F.; Lear, J. D. *Biophys. J.* **2002**, *83*, 1613–1619.  
 (46) Ben-Tal, N.; Honig, B.; Bagdassarian, C. K.; Ben-Shaul, A. *Biophys. J.* **2000**, *79*, 1180–1187.  
 (47) Seelig, A.; Seelig, J. *Biochemistry* **1974**, *13*, 4839–4845.

and bilayers (about 1.3 kcal/mol),<sup>12</sup> we can estimate the maximum concentration (or minimum peptide/detergent ratio) to abolish the pVVVV association in micelles and bilayers. In the case of bilayers, the concentration is estimated at 15.5 mM (a peptide/lipid ratio of 1:150) by  $\Delta G^\circ + \Delta G_{\text{rot/trans}} = k_B T \ln C$ , where  $\Delta G^\circ = -5.5$  kcal/mol. In the case of micelles, the concentration is estimated at 135.3 mM (a peptide/detergent ratio of 1:17) by  $\Delta G^\circ + \Delta G_{\text{rot/trans}} + \Delta G_{\text{b-m}} = k_B T \ln C$ , where  $\Delta G^\circ = -5.5$  kcal/mol. Experimentally, Choma et al. used a peptide/detergent ratio of 1:200 or 1:500 and showed that the association of MS1 disappeared when Asn was replaced by Val,<sup>7</sup> which agrees well with our estimates, given the consideration of the calculation errors.

**Association Mechanism.** The present umbrella sampling MD simulations also provide various structural information on helix–helix and helix–lipid interactions as a function of  $r_{\text{HH}}$ , which helps us propose a TM helix association mechanism. The time-averaged helicity of each peptide remains more than 90% (mostly 95%) at any  $r_{\text{HH}}$ , reflecting that a helix itself, regardless of its association state, is a stable structural motif in membranes (data not shown). The distributions of the helix–helix crossing angles and helix tilt angles are shown in Figure S4 (Supporting Information). The relative orientation (crossing angle) between the two helices is quite restricted while Asn H-bonds exist, but the two helices become uncorrelated beyond  $r_{\text{HH}} = 12$  Å (broader crossing angle and larger tilt angles). The pVNVV peptides in the DMPC membrane appear to have average tilt angles of  $\sim 30^\circ$ , with a relatively wide distribution at  $r_{\text{HH}} \geq 12$  Å.

Putting all the energetic and structural information together, the association mechanism of two pVNVV peptides can be recapitulated as follows: (i) when  $r_{\text{HH}} > 18$  Å, the two helices move independently without specific preference for helix–helix interactions; (ii) when  $15$  Å  $< r_{\text{HH}} < 18$  Å, the two helices start to “feel” each other and the lipids between the helices start to move out; (iii) when  $12$  Å  $< r_{\text{HH}} < 15$  Å, the attractive helix–helix interactions exceed the repulsive helix–lipid interactions that result from the unfavorable helix–lipid enthalpic contribution and the favorable helix–lipid entropic contribution; (iv) at  $r_{\text{HH}} \approx 12$  Å, the bifurcated H-bond between two Asn residues plays an important role to provide specific interactions and to define proper orientation; and (v) the proper orientation induces close packing with the attractive packing energy in the helix–helix interface and inter-peptide Asn-backbone H-bonding at  $r_{\text{HH}} \approx 9.5$  Å.

**Implications in Membrane Protein Folding.** In a simplified view, one may envision membrane protein folding as an overall process of insertion, folding, tilt, rotation, and assembly of TM helices. After insertion, probably via partial or nearly complete folding at the membrane interface,<sup>48,49</sup> individual helices may

have specific thermally accessible tilt and rotation angles in biological membranes. Our recent study demonstrates that the thermally accessible tilt angles of a TM helix in membranes are determined by both the intrinsic entropy contribution arising from the helix precession around the membrane normal and the sequence- and length-specific helix–membrane interactions.<sup>29</sup> The assembly of TM helices clearly depends on delicate helix–helix and helix–membrane interactions as well as the peptide concentration. The present study shows that the contribution from helix–lipid interactions to TM helix association arises from competing forces between unfavorable helix–lipid enthalpic interactions ( $\Delta H^{\text{HL}}$ ) and favorable helix–lipid entropic contributions ( $T\Delta S^{\text{HL}}$ ), i.e., the so-called lipophobic effect.<sup>50</sup> In the case of pVNVV, the overall helix–lipid contribution appears to be repulsive, i.e.,  $T\Delta S^{\text{HL}} < \Delta H^{\text{HL}}$ , which competes with the favorable helix–helix interactions that arise from the specific contribution from the interfacial residues and the generic contribution from the noninterfacial residues. However, it should be stressed that the relative magnitude of each contribution may depend on a specific peptide sequence.

## Conclusions

We have described the role of H-bonding and helix–lipid interactions in TM helix association on the basis of the PMF calculations and the mean force decomposition from umbrella sampling MD simulations of pVNVV and its mutant pVVVV in DMPC membranes. On the basis of the structural and energetic analyses, we also proposed a possible TM helix association mechanism and described its implications in membrane protein folding.

**Acknowledgment.** We are grateful to Charles Brooks, III, and Robert Weaver for valuable comments and suggestions. We thank Richard Pastor and Jeffery Klauda for providing an equilibrated DMPC lipid coordinate. W.I. is a 2007 Alfred P. Sloan Research Fellow. This work was supported by institutional funding from the University of Kansas.

**Supporting Information Available:** Complete ref 18; detailed information on each equilibration step; comparison of Asn H-bonds contribution; decompositions of the helix–lipid contribution; distribution of helix–helix crossing angles and helical tilt angles. This material is available free of charge via the Internet at <http://pubs.acs.org>.

JA711239H

(48) Im, W.; Brooks, C. L., III *Proc. Natl. Acad. Sci. U.S.A.* **2005**, *102*, 6771–6776.

(49) Tang, J.; Signarvic, R. S.; DeGrado, W. F.; Gai, F. *Biochemistry* **2007**, *46*, 13856–13863.

(50) Jähnig, F. *Proc. Natl. Acad. Sci. U.S.A.* **1983**, *80*, 3691–3695.

(51) MacCallum, J. L.; Tieleman, D. P. *J. Am. Chem. Soc.* **2006**, *128*, 125–130.

(52) Armen, R. S.; Uitto, O. D.; Feller, S. E. *Biophys. J.* **1998**, *75*, 734–744.